Surface Enthalpies of Nanophase ZnO with Different Morphologies

Peng Zhang,[†] Fen Xu,[†] Alexandra Navrotsky,*[,†] Jong Soo Lee,[‡] Sangtae Kim,[‡] and Jun Liu[§]

NEAT ORU and Peter A. Rock Thermochemistry Laboratory, University of California at Davis, One Shields Avenue, Davis, California 95616, Department of Chemical Engineering and Materials Science, University of California at Davis, One Shields Avenue, Davis, California 95616, and Pacific Northwest National Laboratory, 902 Battelle Boulevard, Box 9999, Richland, Washington 99352

Received May 2, 2007. Revised Manuscript Received July 25, 2007

A direct calorimetric measurement of the dependence of the surface enthalpy of nanophase ZnO on morphology is reported. Nanoparticles, nanoporous composites, nanorods, and nanotetrapods were prepared with various sizes, and their surface enthalpies were derived from their drop solution enthalpies in molten sodium molybdate. Water adsorption calorimetry for nanoparticles and nanorods was carried out to characterize the stabilization effect of surface hydration. The surface enthalpies of hydrated surfaces for nanoparticles, nanoporous composites, nanorods, and nanotetrapods are 1.31 ± 0.07, 1.42 ± 0.21, 5.19 ± 0.56, and 5.77 ± 2.50 J/m^2, respectively, whereas those of the anhydrous surfaces are 2.55 ± 0.23, 2.74 ± 0.16, 6.67 ± 0.56, and 7.28 ± 2.50 J/m^2, respectively. The surface enthalpies of nanoparticles are the same as those of nanoporous composites and are much lower than those of nanorods and nanotetrapods, which also are close to each other. The dependence of surface enthalpy on morphology is discussed in terms of exposed surface structures. This is the first time that calorimetry on nanocrystalline powders has been able to detect differences in surface energetics of materials having different morphologies.

Introduction

Zinc oxide (ZnO), a wide band gap (3.37 eV) semiconductor with large exciton binding energy (∼60 meV), has attracted great interest because of its potential high-tech applications. ZnO nanoparticles and nanorods/wires have been intensively studied for promising applications as gas sensors,[1] photodetectors,[2] and biomedical[3] and optoelectronic devices.[4,5] Various synthetic methods, such as growth from solution,[6] hydrothermal growth,[7] and thermal evaporation,[8] were widely explored to prepare ZnO nanocrystals. In addition to the nanoparticles, nanoporous composites, nanorods, and nanotetrapods, which will be discussed in this paper, various other morphologies have been observed.[6,8,9] For controlling the morphologies, different surfactants, solvents, pH values, temperatures, and pressures are used. The basic strategy is to control the growth direction and growth speed on the basis of the difference in surface energies of certain planes.[7,10] Nanocrystalline materials with different morphologies and different crystalline surfaces are expected to have different energy states that determine their surface activity and many other chemical and physical properties. Therefore, the determination of such surface energies is essential for both synthesis and applications of ZnO.

The rapidly growing field of ZnO nanostructures begs for experimental benchmarks of their thermodynamic properties. However, reliable experimental data on the energies of ZnO nanocrystal surfaces have not yet been reported[11] because of the difficulty inherent in such measurements. Recently, high-temperature oxide melt solution calorimetry[12] has been shown to be a powerful tool for studying the surface enthalpies of nanophase oxides, such as nanoparticles of Al_2O_3,[13] TiO_2,[14] ZrO_2,[15] and α-Fe_2O_3.[16] In those studies, the particles were roughly spherical or equate in shape, and presumably, a large variety of surfaces were exposed. Thus, an average surface energy was derived for particles grown from aqueous solutions, generally without additives to control morphology. The control of ZnO morphology, to produce particles with significantly different exposed surfaces, offers

* To whom correspondence should be addressed. E-mail: anavrotsky@ucdavis.edu; phone: (530) 752−3292; Fax: (530) 752−9307.

[†] NEAT ORU and Peter A. Rock Thermochemistry Laboratory, University of California at Davis.

[‡] Department of Chemical Engineering and Materials Science, University of California at Davis.

[§] Pacific Northwest National Laboratory.

(1) Katsarakis, N.; Bender, M.; Cimalla, V.; Gagaoudakis, E.; Kiriakidis, G. *Sens. Actuators B: Chem.* **2003**, *96* (1−2), 76−81.
(2) Harnack, O.; Pacholski, C.; Weller, H.; Yasuda, A.; Wessels, J. M. *Nano Lett.* **2003**, *3* (8), 1097−1101.
(3) Al-Hilli, S. M.; Al-Mofarji, R. T.; Willander, M. *Appl. Phys. Lett.* **2006**, *89*, 173119.
(4) Wang, Z. L. *Adv. Mater.* **2000**, *12* (17), 1295-+.
(5) Hu, J. T.; Odom, T. W.; Lieber, C. M. *Acc. Chem. Res.* **1999**, *32* (5), 435−445.
(6) Greene, L. E.; Yuhas, B. D.; Law, M.; Zitoun, D.; Yang, P. D. *Inorg. Chem.* **2006**, *45* (19), 7535−7543.
(7) Cheng, B.; Samulski, E. T. *Chem. Commun.* **2004**, *8*, 986−987.
(8) Yi, G. C.; Wang, C. R.; Park, W. I. *Semicond. Sci. Technol.* **2005**, *20* (4), S22−S34.
(9) Ozgur, U.; Alivov, Y. I.; Liu, C.; Teke, A.; Reshchikov, M. A.; Dogan, S.; Avrutin, V.; Cho, S. J.; Morkoc, H. *J. Appl. Phys.* **2005**, *98* (4), 041301.
(10) Cao, H. L.; Qian, X. F.; Gong, Q.; Du, W. M.; Ma, X. D.; Zhu, Z. K. *Nanotechnology* **2006**, *17* (15), 3632−3636.
(11) Greene, L. E.; Law, M.; Tan, D. H.; Montano, M.; Goldberger, J.; Somorjai, G.; Yang, P. D. *Nano Lett.* **2005**, *5* (7), 1231−1236.
(12) Navrotsky, A. *Phys. Chem. Miner.* **1997**, *24* (3), 222−241.
(13) McHale, J. M.; Auroux, A.; Perrotta, A. J.; Navrotsky, A. *Science* **1997**, *277* (5327), 788−791.
(14) Levchenko, A. A.; Li, G. S.; Boerio-Goates, J.; Woodfield, B. F.; Navrotsky, A. *Chem. Mater.* **2006**, *18* (26), 6324−6332.
(15) Ushakov, S. V.; Navrotsky, A. *Appl. Phys. Lett.* **2005**, *87* (16), 164103.
(16) Mazeina, L.; Navrotsky, A. *Chem. Mater.* **2007**, *19* (4), 825−833.

10.1021/cm0711919 CCC: $37.00
Published on Web 10/13/2007

Table 1. XRD, TEM, AND BET Sizes (nm) of Nanoparticle Samples

sample ID	XRD crystallite size	TEM size	BET size
nanoparticle (P1)	38.3 ± 1.7	36.5 ± 3.3	40.3 ± 0.8
nanoparticle (P2)	26.7 ± 1.5	25.8 ± 4.9	29.4 ± 0.4
nanoparticle (P3)	20.6 ± 0.5	21.8 ± 2.1	35.9 ± 0.7
nanoparticle (P4)	18.3 ± 1.4	20.0 ± 2.1	25.8 ± 0.8
nanoparticle (P5)	21.1 ± 0.5	15.0 ± 1.1	27.2 ± 0.7
nanoparticle (P6)	14.0 ± 0.4	14.3 ± 1.5	25.5 ± 0.4

an opportunity for direct calorimetric measurement of the variation of surface energy with morphology. Thus, the aim of this study is to explore whether such effects can be detected by taking advantage of the large variation of morphology possible for ZnO nanocrystals. Thus, our present work addresses the surface energy of nanophase ZnO with various morphologies, which are obtained by measuring the heat of drop solution of the samples as a function of their surface area.[13,17−19] Because the heat effect associated with water removal needs to be known accurately, water adsorption calorimetry is also performed on ZnO nanoparticles and nanorods. The results are used in the calculation of surface enthalpies of the anhydrous surface. The calorimetric data are discussed in terms of surface structures and are compared to values obtained from computational studies. Calorimetric measurements of the energy of different single-crystal surfaces are not possible because the surface area would be too small for accurate measurement. Thus, the present experiments offer, for the first time, a direct comparison between measured enthalpies and those predicted for different crystallographic planes by various computational methods.

Experimental Procedures

Chemicals and Synthesis. Zinc acetate ($Zn(CH_3COO)_2{\cdot}2H_2O$), tetramethylamine hydroxide (25% in methanol solution), sodium hydroxide (NaOH), $Zn(NO_3)_2{\cdot}xH_2O$, ethanol (CH_3CH_2OH), and ethylenediamine (EDA) were purchased from Alfa Aesar (Ward Hill, MA) and were used without further purification. Lithium hydroxide (LiOH), $HO(CH_2CH_2O)_{20}(CHCH_3CH_2O)_{70}(CH_2CH_2O)_{20}$-OH (designated $EO_{20}PO_{70}EO_{20}$, Pluronics P-123 BASF), and 2-aminoethanesulfonic acid (Taurine, $C_2H_7NO_3S$), were purchased from Aldrich and were used without further purification. Bulk ZnO powder was obtained from commercial ZnO powder (99.99%, Alfa Aesar) and was calcined at 950 °C.

For preparation of ZnO nanoparticles, hydrothermal methods were used.[20] A 1.098 g portion of $Zn(CH_3COO)_2{\cdot}2H_2O$ was dissolved in 10 mL methanol and mixed with 20 mL of tetramethylamine hydroxide (25% in methanol solution). The resulting solution was placed in a Teflon-lined stainless steel autoclave and was heated at 75 °C for 1 day. To obtain various sized ZnO nanoparticles, zinc acetate solutions in methanol were mixed with tetramethylammonium hydroxide solution at different molar ratios. These mixtures were treated under hydrothermal conditions for different periods of time. The sizes of nanoparticles range from 14 to 40 nm (see Table 1).

The synthesis of a porous nanocomposite of ZnO involves the functionalization of the premade colloidal ZnO nanocrytallites, followed by self-assembly under the assistance of copolymers. A detailed description of the synthesis is found elsewhere.[21]

For the preparation of nanorods, 0.005 mol of $Zn(NO_3)_2$ were dissolved in 10 mL of a NaOH solution with a Zn^{2+}:OH^- ratio of 1:30, and then the mixture was diluted with 100 mL of pure ethanol. After 5 mL of ethylenediamine (EDA) were added to the mixture, it was stirred at room temperature for 7−11 days to obtain different sizes.[22] Another solution route was to dissolve $Zn(CH_3COO)_2{\cdot}2H_2O$ in methanol and to heat the solution to 65 °C. A solution of KOH in methanol was then added to a zinc acetate solution, and the system was refluxed. Nanorods about 10 nm in diameter and up to 200 nm in length were produced by this route. Hydrothermal treatment of $Zn(CH_3COO)_2{\cdot}2H_2O$ and a NaOH solution (Zn:OH = 1:4) with the assistance of poly(ethylene glycol) (PEG400) was also used to prepare nanorods.[23] The diameters of the as-prepared ZnO nanorod samples range from 10 to 30 nm, and the aspect ratios range from 3 to 30.

ZnO tetrapods were synthesized using a thermal evaporation method. An alumina boat containing commercial ZnO powder (Aldrich, 99.99%) was loaded into the center of an alumina tube (Ø 3 × L 40 in.) horizontally placed in a conventional tube furnace. Silicon substrates (5 × 5 mm^2) were placed at the downstream end of the tube to grow ZnO tetrapods. The ZnO powder was evaporated at 1400 °C for 2 h. The temperature of the substrates placed at the downstream end of the alumina tube was monitored to be about 650 °C. High-purity argon gas serving as a mass-transporting medium was fed at a flow rate of 500 mL/min into the alumina tube. The chamber pressure was maintained at 0.5 atm.

Characterization. Phase identification was carried out by powder X-ray diffraction (XRD) using a Scintag PAD V diffractometer (Cu Kα radiation) operated at 45 kV and 40 mA with a 0.02° step size and 3−5 s dwell time. The XRD patterns were analyzed by using the Jade program (version 6.11, 2002; Materials Data Inc., Livermore, CA) to calculate the size of the nanoparticles. The morphologies of the samples were observed using a Philips CM-12 transmission electron microscope (TEM) operating at 100 kV. The specimens for TEM observation were prepared by dispersing the sample in ethanol and then deposing on a molybdenum grid.

The specific surface areas were measured by N_2 adsorption at 77 K using a 5-point Brunauer−Emmett−Teller (BET) technique on the analysis port of a Micromeritics ASAP 2020 (Micromeritics Instrument Corporation, Norcross, GA) in the P/P_0 range 0.05−0.3. Prior to analysis, the samples were made into 5 mg pellets and degassed at 300 °C for 3−4 h. However, in the case of nanoparticles, when the X-ray nanocrystallite size is smaller than 25 nm, the size calculated from the BET surface area (assuming spherical particles) appears to be larger than those from XRD and TEM (see Table 1). The reason may be the easy coagulation of ZnO polar nanoparticles, which makes some surfaces unreachable by nitrogen gas. Therefore, we chose, for further calculation, the largest surface area among these three sources if they were different. For nanoporous composites, nanorods, and nanotetrapods, the BET surface area was the only reliable source of surface area measurement because of their special morphologies and larger sizes (>25 nm), so we used BET surface areas in the calculations.

After BET analysis, the sample was transferred into an argon-filled glove box (O_2 and H_2O levels of <1 ppm) for storage. The

(17) Mazeina, L.; Deore, S.; Navrotsky, A. *Chem. Mater.* **2006**, *18* (7), 1830−1838.
(18) Ranade, M. R.; Navrotsky, A.; Zhang, H. Z.; Banfield, J. F.; Elder, S. H.; Zaban, A.; Borse, P. H.; Kulkarni, S. K.; Doran, G. S.; Whitfield, H. J. *Proc. Natl. Acad. Sci., U.S.A.* **2002**, *99*, 6476−6481.
(19) Pitcher, M. W.; Ushakov, S. V.; Navrotsky, A.; Woodfield, B. F.; Li, G. S.; Boerio-Goates, J.; Tissue, B. M. *J. Am. Ceram. Soc.* **2005**, *88* (1), 160−167.
(20) Cheng, B.; Shi, W. S.; Russell-Tanner, J. M.; Zhang, L.; Samulski, E. T. *Inorg. Chem.* **2006**, *45* (3), 1208−1214.
(21) Xu, F.; Zhang, P.; Navrotsky, A.; Yuan, Z.-Y.; Ren, T.-Z.; Halasa, M.; Su, B.-L. *Chem. Mater.* **2007**, in press.
(22) Liu, B.; Zeng, H. C. *Langmuir* **2004**, *20* (10), 4196−4204.
(23) Li, Z. Q.; Xiong, Y. J.; Xie, Y. *Inorg. Chem.* **2003**, *42* (24), 8105−8109.

Table 2. Characterization and Thermochemical Data for ZnO

sample ID	surface area ($10^3 m^2$/mol)	water content x in $ZnO \cdot xH_2O$	ΔH_{ds} (kJ/mol) measured for $ZnO \cdot xH_2O$	corrected for ZnO[a]	corrected for ZnO[b]
bulk	0	0	16.49 ± 0.15	16.49 ± 0.15	16.49 ± 0.15
nanoparticle (P1)	2.23	0.0300 ± 0.0013	15.08 ± 0.32	13.00 ± 0.33	9.80 ± 0.46
nanoparticle (P2)	3.20	0.0189 ± 0.0010	15.97 ± 0.49	12.59 ± 0.50	8.14 ± 0.58
nanoparticle (P3)	4.14	0.0448 ± 0.0013	13.70 ± 0.55	10.61 ± 0.56	4.63 ± 0.68
nanoparticle (P4)	4.66	0.0448 ± 0.0043	13.17 ± 0.54	10.08 ± 0.62	3.49 ± 1.46
nanoparticle (P5)	5.69	0.0337 ± 0.0013	11.49 ± 0.47	9.16 ± 0.48	3.69 ± 0.66
nanoparticle (P6)	6.09	0.0684 ± 0.0015	13.04 ± 0.38	8.32 ± 0.39	−0.51 ± 0.61
nanoporous (PO1)	1.57	0.0136 ± 0.0031	15.89 ± 0.32	14.95 ± 0.38	12.80 ± 1.07
nanoporous (PO2)	2.96	0.0637 ± 0.0026	16.20 ± 0.33	11.80 ± 0.38	8.67 ± 0.58
nanoporous (PO3)	3.26	0.0503 ± 0.0022	15.13 ± 0.24	11.66 ± 0.28	7.13 ± 0.56
nanoporous (PO4)	3.71	0.0334 ± 0.0023	14.27 ± 0.23	11.96 ± 0.28	6.81 ± 0.77
nanorod (R1)	0.49	0.0563 ± 0.0022	15.08 ± 0.41	13.70 ± 0.41	12.96 ± 0.48
nanorod (R2)	0.77	0.0480 ± 0.0016	14.10 ± 0.37	10.78 ± 0.37	9.62 ± 0.51
nanorod (R3)	1.13	0.0170 ± 0.0030	13.40 ± 0.32	12.22 ± 0.32	10.52 ± 0.83
nanorod (R4)	2.24	0.0675 ± 0.0014	8.91 ± 0.31	4.25 ± 0.31	0.83 ± 0.44
nanorod (R5)	2.34	0.0380 ± 0.0030	6.84 ± 0.45	4.22 ± 0.45	0.67 ± 0.85
tetrapod (T1)	1.43	0.0143 ± 0.0024	12.32 ± 0.48	11.33 ± 0.48	9.18 ± 0.97
tetrapod (T2)	1.79	0.0484 ± 0.0058	7.96 ± 1.96	4.62 ± 1.96	1.90 ± 2.31

[a] Corrected on the basis of the enthalpy of liquid water. [b] Corrected on the basis of the enthalpy of water adsorption.

water content of each sample used for the drop solution calorimetry was determined by thermogravimetry (TG) on a Netzsch STA 449 system. The sample pellets (~30 mg) were heated from room temperature to 1000 °C at 10 °C/min under a flow of dry oxygen at 40 mL/min.

High-Temperature Oxide Melt Solution Calorimetry. Calorimetry was performed on a custom-built Calvet twin microcalorimeter[12] using sodium molybdate ($3Na_2O \cdot 4MoO_3$) melt at 700 °C as solvent. Oxygen was flushed through the calorimeter at ~35 mL/min to maintain the oxidizing conditions and to remove the evolved moisture. Oxygen bubbling though the solvent at ~5 mL/min was also used to agitate the solvent to aid dissolution. The sample pellets (~5 mg) were weighed and stored in a small vial in the glovebox and were exposed to air for only a few seconds before being dropped from room temperature into the molten solvent (700 °C) in the calorimeter. The procedure is now standard and has been described previously.[12] The measured drop solution enthalpy includes heat content of sample and adsorbed water, heat of dissolution, and heat of dehydration.

Water Adsorption Calorimetry. Enthalpies of water adsorption were measured at room temperature using a Calvet microcalorimeter, Setaram DSC-111, (Setaram Instruments, Lyon, France) coupled with a Micromeritics ASAP 2020 analysis system.[15] This combined system enables precise gas dosing, volumetric detection of amount of adsorbed water, and simultaneous measurement of heat effect.[15] Sample pellets were placed in one side of a quartz forked tube and degassed under a static vacuum ($<10^{-5}$ Torr) at 450 °C for at least 6 h to remove most of water from the surface. After the measurement of the surface area for the sample and the free space of the tube, the system was evacuated again until the sample leak rate was <0.6 μm Hg/min. Then, a series of precisely controlled small doses of gaseous water was released into the system at room temperature until P/P_0 reached ~0.25. The adsorption heat of each dose generated an exothermic calorimetric peak. The simultaneous record of the amount of adsorbed water and the adsorption enthalpy provided a high-resolution measurement of differential heat of adsorption as a function of surface coverage.[15]

Results

The XRD patterns of all the samples show the wurtzite structure with broadened peaks. Table 2 lists the surface area, water content, measured heat of drop solution ΔH_{ds},[12] and calculated thermodynamic parameters for all samples. The ΔH_{ds} of the nanocrystals is less endothermic than that of bulk ZnO. This arises from their positive surface energy, as expressed in the following equation (eq 1),

$$\Delta H_{ds}(\text{nano} \rightarrow \text{soln}) = -A\gamma + \Delta H_{ds}(\text{bulk} \rightarrow \text{soln}) \quad (1)$$

where A is the surface area (m^2/mol) and γ is the surface enthalpy (J/m^2) of nanocrystals. The surface area, measured by BET and/or calculated from the XRD and TEM size, is known for all samples. When ΔH_{ds} is plotted versus surface area (A), a linear fit can be obtained with the negative of the slope being the surface energy (γ).

Because of the significant heat effect associated with the water remaining in all of the samples, the endothermic heat of water removal (x mol H_2O/mol ZnO) from the samples ($ZnO \cdot xH_2O$) was measured by water adsorption experiments. The enthalpies of water adsorption are shown in Figure 1. The differential enthalpy of adsorption (Figure 1a) is strongly exothermic at low coverage and approaches the value for water condensation (−44 kJ/mol) at high coverage. This behavior is similar to that seen for other oxides, Al_2O_3,[13] TiO_2,[14] ZrO_2,[15] and α-Fe_2O_3.[16]

To derive surface enthalpy, we must separate the effect on heat of drop solution of surface area from that of water adsorption. This can be done, conceptually, in two ways, as shown in thermodynamic cycles (Table 3). If one considers the water to be adsorbed with an energy equal to its heat of condensation, then after correction for adsorption of x moles of H_2O per mole of ZnO, the resulting corrected heat of drop solution can be plotted versus the surface area. The data produce the surface enthalpy of the hydrated surface as the slope of the linear fit. This is because any effects associated with differences in energy of water adsorption, resulting from interaction of water with the surface and surface relaxation, are still included in the corrected heat of drop solution. On the other hand, if one uses the measured integral heat of water adsorption (Figure 1b) to correct for the water adsorption enthalpy, then one obtains the surface enthalpy

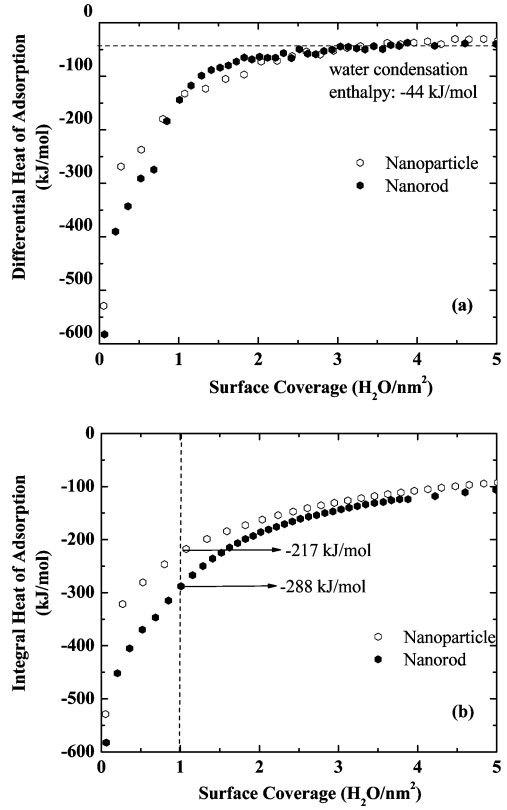

Figure 1. Differential (a) and integral (b) heat of water adsorption of nanoparticles (hollow hexagonal symbols) and nanorods (filled hexagonal symbols) versus water coverage (number of H_2O/nm^2); the dashed lines in panels (a) and (b) represent the enthalpy of vapor condensation at room temperature and the integral heat of adsorption at the coverage of 1.0 H_2O/nm^2.

of the anhydrous surface. This methodology has been discussed previously.[15]

The measured enthalpy of drop solution consists of three contributions: that of bulk ZnO, that of water, and that of the size effect or surface enthalpy. The first two contributions are endothermic, namely, the enthalpy of drop solution of bulk ZnO and the enthalpy of desorbing and heating water, whereas the last, representing a destabilization relative to the bulk material, is exothermic. To illustrate the contribution of each effect, we calculate these effects for the nanopowder samples P1 (38.3 nm) and P5 (15.0 nm). For P1, with a total effect of 184 J/g, 201 J would come from bulk ZnO, 64 J from H_2O, and −81 J from the size effect. For P5 (140 J/g), the contributions are 201, 95, and −156 J, respectively. Thus, the enthalpy related to the size effect is a very substantial portion of the total heat effect measured, and the calorimetric method has the sensitivity to reliably obtain the surface enthalpy.

The surface enthalpies of nanoparticles (enthalpy of hydrated surface $\gamma_{hyd} = 1.31 \pm 0.07$ J/m^2; enthalpy of anhydrous surface $\gamma_{anhyd} = 2.55 \pm 0.23$ J/m^2) agree very well with those of nanoporous composites ($\gamma_{hyd} = 1.42 \pm 0.21$ J/m^2 and $\gamma_{anhyd} = 2.74 \pm 0.16$ J/m^2), as shown in Figure 2, panels a and b. When these calorimetric results are put together, as shown in Figure 2c, surface enthalpies of $\gamma_{hyd} = 1.33 \pm 0.08$ J/m^2 and $\gamma_{anhyd} = 2.60 \pm 0.17$ J/m^2 are obtained. Figure 3a presents the calorimetrically determined surface enthalpy of ZnO nanorods. Within the error ranges, the surface enthalpies of nanorods (Figure 3a, $\gamma_{hyd} = 5.19 \pm 0.56$ J/m^2 and $\gamma_{anhyd} = 6.67 \pm 0.56$ J/m^2) are the same as those of nanotetrapods (Figure 3b, $\gamma_{hyd} = 5.77 \pm 2.50$ J/m^2 and $\gamma_{anhyd} = 7.28 \pm 2.50$ J/m^2). The relatively large uncertainty of the results for nanotetrapods arises from the limited number of data points. Figure 3c shows the combined calorimetric data for both nanorods and nanotetrapods and the combined surface enthalpies ($\gamma_{hyd} = 5.37 \pm 0.77$ J/m^2 and $\gamma_{anhyd} = 6.85 \pm 0.77$ J/m^2). These values are much higher than those of nanoparticles and nanoporous composites. The results are summarized in Table 4.

In all cases, the enthalpy of the sample, corrected for water, falls on a straight line passing very close to the point for pure bulk ZnO at zero surface area. Although the bulk phase was used as a point in the fitting, the linear fit was not constrained to go through it. This argues for there being no significant curvature in the plot of enthalpy versus surface area for surface areas smaller than those of the samples studied. That is, the surface enthalpy is constant for surface areas between zero and the largest value studied for each group of samples. Similar behavior has been seen for other systems, for example, Al_2O_3,[13] TiO_2,[14] ZrO_2,[15] and α-Fe_2O_3.[16] Furthermore, there is overlap in surface area between some of the samples of the nanoparticle/nanoporous group and the nanorod/tetrapod group. For these reasons, we believe that the difference in the surface enthalpy of the two groups of samples arises from their morphologies and not from difference in the size range of the samples in the various groups. At still smaller size (higher surface area), where crystallinity diminishes, it is possible that the relation between enthalpy and surface area may deviate from the straight lines seen for coarser samples, but we have no information on this regime, nor do we have direct information on surface species, dangling bonds, or other defects as a function of size and morphology. The surface enthalpies we report represent values averaged over a variety of surface sites that are present in each sample. Their constancy may suggest that such speciation does not change strongly with size, but this is not a necessary conclusion. The atomistic reasons for the different surface enthalpies are further discussed below.

We have thus shown that the surface enthalpies depend on the morphologies. Here, we are interested in several issues. (1) Why are the surface enthalpies of nanoparticles

Table 3. Thermochemical Cycle for Water Adsorption Correction

(1) $ZnO{\cdot}xH_2O$ (nano, 298 K) → ZnO (soln, 973 K) + xH_2O (g, 973 K)	$\Delta H1 = \Delta H_{ds}$
(2) H_2O(g, 973 K) → H_2O (g, 298 K)	$\Delta H2 = -25.0 \pm 0.1$ kJ/mol
(3) ZnO (nano, 298 K) + xH_2O (g, 298 K) → $ZnO{\cdot}xH_2O$ (nano, 298 K)	$\Delta H3 = x\Delta H_{ads}$
(4) ZnO(nano, 298 K) → ZnO (soln, 973 K)	$\Delta H4 = \Delta H_{corr}$

$\Delta H4 = \Delta H1 + x\Delta H2 + \Delta H3$

ΔH_{corr} (hydrated) $= \Delta H_{ds} + x\Delta H2 + x(-44.0 \pm 0.1$ kJ/mol)

ΔH_{corr} (anhydrous) $= \Delta H_{ds} + x\Delta H2 + x\Delta H_{ads}$

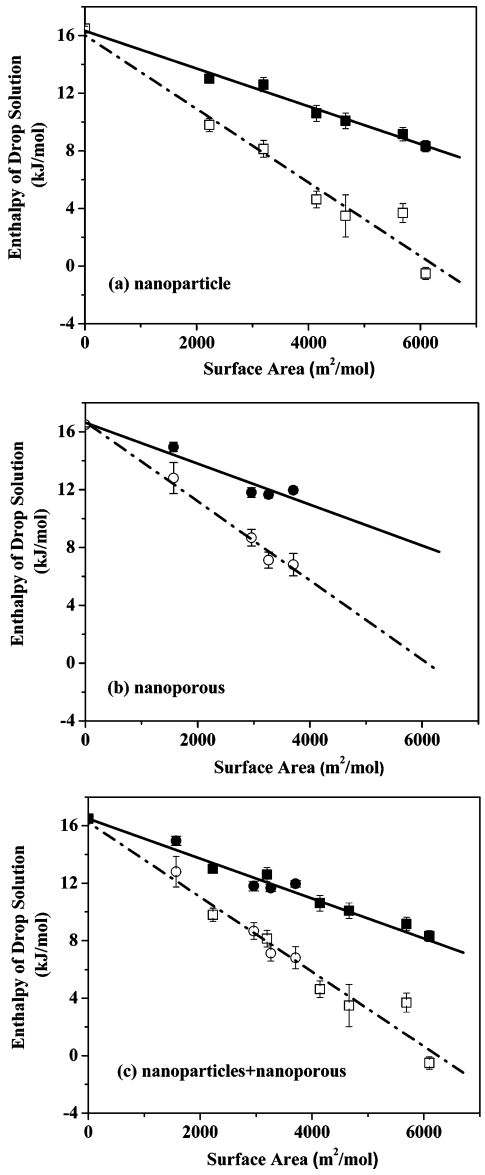

Figure 2. Drop solution enthalpies of ZnO nanoparticles (symbol: square) and nanoporous composites (symbol: circle) versus surface area. Filled symbols and solid line represent data and fits using a water correction based on the enthalpy of pure H_2O. Open symbols and dot-dashed lines represent data and fits using a water correction based on the enthalpy of water adsorption. The slopes of the fits represent the surface enthalpies of the hydrated and anhydrous surfaces. (a) nanoparticles: $\gamma_{hyd} = 1.31 \pm 0.07$ J/m^2, $R^2 = 0.99$; $\gamma_{anh} = 2.55 \pm 0.23$ J/m^2, $R^2 = 0.96$. (b) nanoporous: $\gamma_{hyd} = 1.42 \pm 0.21$ J/m^2, $R^2 = 0.92$; $\gamma_{anh} = 2.74 \pm 0.16$ J/m^2, $R^2 = 0.99$. (c) combination of nanoparticle and nanoporous: $\gamma_{hyd} = 1.33 \pm 0.08$ J/m^2, $R^2 = 0.97$; $\gamma_{anh} = 2.60 \pm 0.17$ J/m^2, $R^2 = 0.96$. The linear fits and uncertainties are given by the fitting program. Error bars, when not shown, are smaller than the size of the symbol.

(both anhydrous and hydrated surfaces) the same as those of nanoporous composites? (2) Similarly, why are the surface enthalpies of nanorods and nanotetrapods the same? (3) For all of the morphologies, the surface enthalpies of anhydrous surfaces are about 1.3−1.5 J/m^2 higher than those of hydrated surfaces. How does this relate to the stabilization effect of surface hydration? In the following section, we discuss these points in detail.

Discussion

Figure 4 shows schematic morphologies of ZnO nanoparticles, nanoporous composites, nanorods, and nanotetrapods.

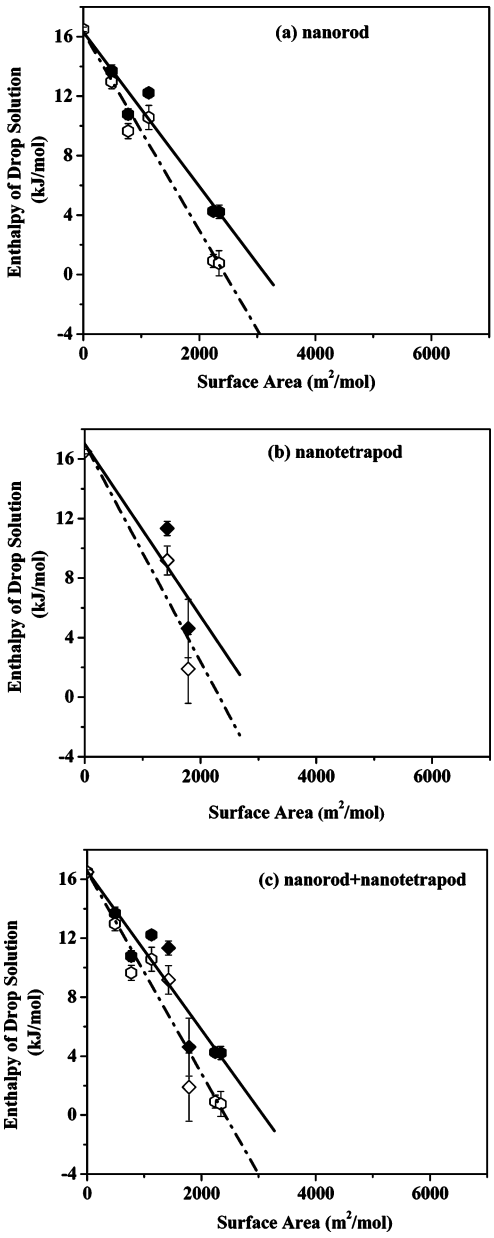

Figure 3. Drop solution enthalpies of ZnO nanorods (symbol: hexagon) and nanotetrapods (symbol: diamond) versus surface area. Filled symbols and solid line represent data and fits using a water correction based on the enthalpy of pure H_2O. Open symbols and dot-dashed lines represent data and fits using a water correction based on the enthalpy of water adsorption. The slopes of the fits represent the surface enthalpies of the hydrated and anhydrous surfaces. (a) nanorods: $\gamma_{hyd} = 5.19 \pm 0.56$ J/m^2, $R^2 = 0.96$; $\gamma_{anh} = 6.67 \pm 0.56$ J/m^2, $R^2 = 0.97$. (b) nanotetrapods: $\gamma_{hyd} = 5.77 \pm 2.50$ J/m^2, $R^2 = 0.84$; $\gamma_{anh} = 7.28 \pm 2.50$ J/m^2, $R^2 = 0.89$. (c) nanorods and nanotetrapods: $\gamma_{hyd} = 5.37 \pm 0.77$ J/m^2, $R^2 = 0.89$; $\gamma_{anh} = 6.85 \pm 0.77$ J/m^2, $R^2 = 0.93$. The linear fits and uncertainties are given by the fitting program. Note that, for ease of comparison, all graphs in Figures 2 and 3 have the same vertical and horizontal scales. Error bars, when not shown, are smaller than the size of the symbols.

For different ZnO morphologies, different planes are exposed, which presumably have different surface enthalpies.

In reality, the exposed surfaces of nanoparticles (Figure 4a) are very complicated and difficult to identify. This is because various planes are exposed on the surface, and they can be highly stabilized by surface reconstruction, relaxation, vacancies, defects, and adsorbents, including H_2O. Therefore, the surface enthalpies for the nanoparticles represent the average values for these stabilized planes.

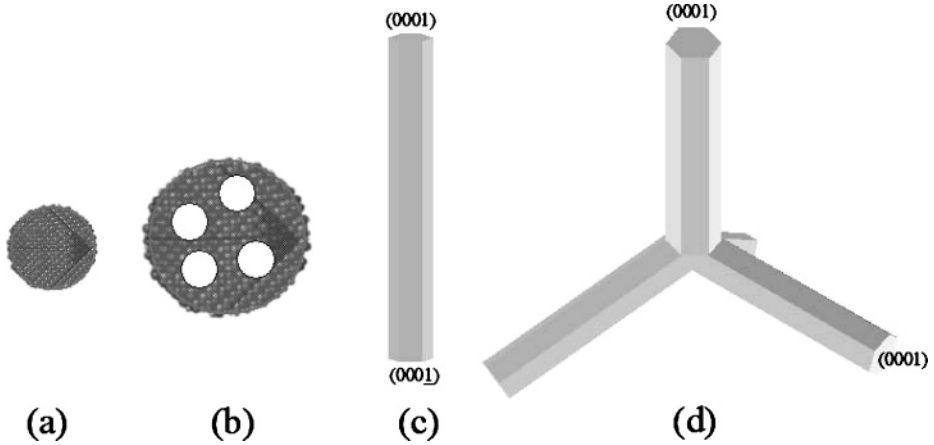

Figure 4. Schematic depiction of ZnO (a) nanoparticle,[37] (b) nanoporous structure,[21] (c) nanorod, and (d) nanotetrapod.

Table 4. Surface Enthalpies of the Nanophase ZnO with Different Morphologies

	surface enthalpy (J/m^2)	
morphology	hydrated surface	anhydrous surface
nanoparticles	$1.31 + 0.07$	2.55 ± 0.23
nanoporous	1.42 ± 0.21	2.74 ± 0.16
nanoparticle + nanoporous	1.33 ± 0.08	2.60 ± 0.17
nanorods	5.19 ± 0.56	6.67 ± 0.56
tetrapods	5.77 ± 2.50	7.28 ± 2.50
nanorods + tetrapods	5.37 ± 0.77	6.85 ± 0.77

Nanoporous ZnO has been shown to be a crystallized assemblage of nanoparticles created by the synthetic strategy.[21] The structure of these porous composites is shown in Figure 4b. The composites contain several nanoscale pores in a single nanoparticle plus pores connecting particles. The particle is formed by the coalescence of smaller surfactant-modified nanocrystallites. After the surfactants are removed, the nanoscale pores are left in the particle, and the interfaces among the smaller precursor particles probably disappear during recrystallization.

Therefore, the surfaces of the precursor crystallites comprise the exposed surface of these nanoporous composites. The surface structure of the precursors is thus kept by the porous composites if there are no major structure changes on these surfaces during the synthesis process. This picture is supported by our calorimetric results. The measured surface enthalpies of nanoporous composites are the same as those of nanoparticles.

Nanorods and nanotetrapods display different surface planes and surface enthalpies. Compared to the complicated surface structure of the nanoparticles that might be highly stabilized by various mechanisms, the surface of the nanorods is relatively simple and uniform (Figure 4c), and only certain planes are exposed. It is known that ZnO has a distorted wurtzite structure consisting of hexagonal Zn and O planes alternately stacked along its *c*-axis. The nanorods are grown along the *c*-axis and are terminated with the polar $\pm(0001)$ planes. In this paper, we call the enclosing planes parallel to the *c*-axis "*c*-axis parallel planes". They reflect the hexagonal symmetry (C_6) and are identified as the nonpolar $\{10\bar{1}0\}$ planes[6,24−26] or the $\{11\bar{2}0\}$ planes.[27] A nanotetrapod can be viewed as an assembly of four nanorods joined from their $-(0001)$ sides, as shown in Figure 4d. Thus, the morphology of nanotetrapods is very similar to that of nanorods, with only the region of joining, which represents only a small part of the sample, possibly having a different structure, namely zinc blende.[28] The surface enthalpies of these two structures are thus expected to be similar, which is supported by our calorimetric results. This can explain an experimental observation that nanorods are often formed in the preparation of nanotetrapods.[29] Because the contribution of the polar surfaces to the total surface area is small (less than 5% of total surface area for a nanorod with an aspect ratio of 10), the exposed surface planes of both nanorods and tetrapods are mainly *c*-axis parallel planes. The surface enthalpies of nanorods and nanotetrapods ($\gamma_{hyd} = 5.37 \pm 0.77$ J/m^2 and $\gamma_{anhyd} = 6.85 \pm 0.77$ J/m^2) are thus dominated by the energetics of these planes.

It is interesting that nanorods and nanotetrapods show higher surface enthalpy than that of nanoparticles. According to ab initio calculations, the $\{10\bar{1}0\}$ planes with cleavage energy of 2.3 J/m^2 are the most stable among the ZnO crystalline planes,[30−32] whereas the cleavage energy of $\{11\bar{2}0\}$ planes is estimated to be 2.5[33] or 4.1 J/m^2, which may be even higher than that of the polar $\pm(0001)$ planes (4.0 J/m^2).[30] Therefore, if the nanorod surfaces are dominated by $\{11\bar{2}0\}$ planes and their cleavage energy is higher than that of the polar surfaces, then the surface energy of nanorods would indeed be higher than that of nanoparticles. On the other hand, if their surfaces are dominated by the $\{10\bar{1}0\}$ planes, and these are indeed the most stable, as the ab initio calculations suggest, then the nanorods would be more stable

(24) Liu, B.; Zeng, H. C. *J. Am. Chem. Soc.* **2003**, *125* (15), 4430−4431.
(25) Ding, Y.; Wang, Z. L. *J. Phys. Chem. B* **2004**, *108* (33), 12280−12291.
(26) Yan, Y.; Al-Jassim, M. M.; Wei, S. H. *Phys. Rev. B* **2005**, *72* (16), 235406.
(27) Wang, Z. L. *J. Phys. Condens. Matter* **2004**, *16* (25), R829−R858.
(28) Ding, Y.; Wang, Z. L.; Sun, T.; Qiu, J. *Appl. Phys. Lett.* **2007**, *90*, 153510.
(29) Cheng, W. D.; Wu, P.; Zou, X. Q.; Xiao, T. *J. Appl. Phys.* **2006**, *100* (5), 054311.
(30) Wander, A.; Harrison, N. M. *Surf. Sci.* **2000**, *468* (1−3), L851−L855.
(31) Wander, A.; Harrison, N. M. *J. Chem. Phys.* **2001**, *115* (5), 2312−2316.
(32) Wander, A.; Schedin, F.; Steadman, P.; Norris, A.; McGrath, R.; Turner, T. S.; Thornton, G.; Harrison, N. M. *Phys. Rev. Lett.* **2001**, *86* (17), 3811−3814.
(33) Meyer, B.; Marx, D. *Phys. Rev. B* **2003**, *67* (3), 035403.
(34) Spanhel, L.; Anderson, M. A. *J. Am. Chem. Soc.* **1991**, *113* (8), 2826−2833.

than nanoparticles. However, nanorod surfaces also possibly contain defects, including higher index planes with higher surface enthalpies.[25] In synthesis in solution, nanoparticles can crystallize under mild conditions,[34] whereas nanorods are generally grown under more extreme conditions such as hydrothermal synthesis[24] and from strong basic solutions with the help of directive surfactants or ligands.[22,23] Therefore, in reality, nanorods are more difficult to prepare, consistent with their higher surface enthalpy.

Calorimetric surface enthalpies of ZnO nanocrystals are higher than theoretical calculations. The ab initio calculation derived the cleavage energy of ZnO $\pm(0001)$, $(10\bar{1}0)$, and $(11\bar{2}0)$ surfaces to be about 4.0, 2.3, and 2.5 (or 4.1) J/m^2, respectively,[30−32] which indicates a theoretical surface energy of about 2.0, 1.15, and 1.25 (or 2.05) J/m^2, respectively. However, the measured surface enthalpy of *c*-axis parallel planes from nanorods and nanotetrapods ($\gamma_{hyd} = 5.37 \pm 0.77$ J/m^2 and $\gamma_{anhyd} = 6.85 \pm 0.77$ J/m^2) is much higher than these values. The existence of a considerable part of higher-index facets might increase the average surface enthalpy of the nanorods.[25] However, the concentration of any such defects is still unknown because of the limited areas studied by the high-resolution TEM. The discrepancy between the experimental and theoretical surface enthalpies still awaits further investigation.

Usually, when synthesizing ZnO nanocrystals by vapor deposition methods, the as-produced ZnO are only exposed to a gaseous environment or a vacuum. In this case, the surface energy of the anhydrous surface is considered to control the thermodynamics of the growth process. However, under ambient conditions, ZnO surfaces are generally hydrated, and the hydrated surface enthalpy represents the thermodynamics of the surfaces. Thus, when ZnO nanomaterials are involved in coagulation, self-assembly, or Ostwald ripening in an aqueous solution, the processes are driven by enthalpies of hydrated surface. The difference between the surface enthalpies of anhydrous and hydrated surface are 1.27 $\pm$ 0.19 and 1.48 $\pm$ 1.09 J/m^2 for nanoparticles and nanorods, respectively. This difference highlights the stabilization effect of surface hydration. However, how does the surface hydration stabilize the surface, and what is the process of hydration? The results from adsorption calorimetry offer some insights.

The differential enthalpy of water adsorption (kJ/mol) on the surface of nanoparticles (Surface Area, SA = 15.94 m^2/g) and nanorods (SA = 16.85 m^2/g) versus the surface water coverage (water molecules/nm^2) is shown in Figure 1a. The exothermic heat effect of both samples starts from about -550 kJ/mol at low coverage and approaches -44 kJ/mol (enthalpy of water condensation at room temperature) at high coverage. The strongly exothermic initial enthalpy, also seen in systems such as alumina,[13] titania,[14] zirconia,[15] and hematite,[16] is evidence for strongly bound (chemisorbed) water. The approach to -44 kJ/mol indicates that, at the highest water content, the additional water molecules have the energetics of bulk liquid water and are thus physisorbed. The decrease in magnitude of the heat of adsorption with coverage is gradual and not stepwise. This probably reflects the heterogeneity of the assemblage of particles and the complex spectrum of available bonding sites.

On the molecular level, the following processes may be taking place. First, the dangling bonds of the surface zinc atoms are saturated by the oxygen atoms from the first water molecules adsorbed, accompanied by a large exothermic heat effect. The bonded H_2O molecules may totally or partially dissociate.[35] In this way, the ZnO surface is saturated by H_2O or OH groups. Then, after full conversion of such dangling bonds on high-energy sites to more stable configurations, the additional adsorbed water molecules condense on the surface of the H_2O (OH) layers with hydrogen bonding among themselves, and eventually, they behave like liquid water.

We hesitate to describe the adsorption in terms of coverage in specific layers, and we avoid terms such as "first monolayer of adsorbed water". The surfaces are complex and rough, and they consist of a variety of planes, steps, kinks, and defect sites, each providing a different bonding environment. The distribution may vary from particle to particle and for different sample preparations. What we see in the heat of adsorption behavior is an average over this complex assemblage.

As shown in Figure 1a, the adsorption enthalpy of both nanoparticles and nanorods reaches the value for water condensation at a coverage of about 3.0 H_2O/nm^2. The corresponding integral heat of adsorption of nanoparticles and nanorods at this point are -130 ± 3 and -145 ± 3 kJ/mol (Figure 1b), respectively. The TG experiments for the nanoparticle and nanorod samples showed $\sim$3.3 and 2.4 H_2O/nm^2 remained after degassing at 450 °C for 7 h. Therefore, the strongly bound water constitutes a total coverage of about 6.3 and 5.4 H_2O/nm^2 for nanoparticle and nanorods, respectively. The cross section of the water molecules on the surface is thus about 0.17 and 0.18 nm^2, which is close to the average value reported (0.16 nm^2).[14,36] The heat of adsorption for water remaining after degassing at 450 °C is approximated by the integral heat of adsorption at a coverage of 1.0 H_2O/nm^2, as shown in Figure 2b, which are -288 ± 3 and -217 ± 3 kJ/mol for nanoparticles and nanorods, respectively.

Conclusions

For the first time, calorimetric measurements are used to detect differences in surface energetics of nanocrystals having different morphologies. ZnO nanoparticles and nanoporous composites have similar surface enthalpies, which are significantly lower than those of nanorods and tetrapods. Hydrated surfaces have a lower surface enthalpy than anhydrous ones. The enthalpy of water adsorption is strongly exothermic at low coverage.

Acknowledgment. This work was supported by the Department of Energy, grant No. FG-031ER15237.

CM0711919

(35) Meyer, B.; Marx, D.; Dulub, O.; Diebold, U.; Kunat, M.; Langenberg, D.; Woll, C. *Angew. Chem. Int. Ed.* **2004**, *43* (48), 6642−6645.
(36) Hall, P. G.; Langrangoldsmith, H. *J. Phys. Chem.* **1992**, *96* (2), 867−870.
(37) Andelman, T.; Gong, Y. Y.; Polking, M.; Yin, M.; Kuskovsky, I.; Neumark, G.; O'Brien, S. *J. Phy. Chem. B* **2005**, *109* (30), 14314−14318.